Clinical Science (2022) **136** 643–656
https://doi.org/10.1042/CS20211122

PORTLAND PRESS

Research Article

Annexin A1 treatment prevents the evolution to fibrosis of experimental nonalcoholic steatohepatitis

Laila Lavanya Gadipudi[1,*], Naresh Naik Ramavath[1,*], Alessia Provera[1,*], Chris Reutelingsperger[2], Emanuele Albano[1], Mauro Perretti[3,†] and Salvatore Sutti[1,†]

[1]Department of Health Sciences and Interdisciplinary Research Centre for Autoimmune Diseases, University of East Piedmont, Novara, Italy; [2]Cardiovascular Research Institute Maastricht, Department of Biochemistry, Maastricht University, Maastricht, The Netherlands; [3]William Harvey Research Institute, Barts and The London School of Medicine, Queen Mary University of London, U.K.

Correspondence: Emanuele Albano (emanuele.albano@med.unipmn.it)

Annexin A1 (AnxA1) is an important effector in the resolution of inflammation which is involved in modulating hepatic inflammation in nonalcoholic steatohepatitis (NASH). In the present study, we have investigated the possible effects of treatment with AnxA1 for counteracting the progression of experimental NASH.

NASH was induced in C57BL/6 mice by feeding methionine–choline deficient (MCD) or Western diets (WDs) and the animals were treated for 4–6 weeks with human recombinant AnxA1 (hrAnxA1; 1 μg, daily IP) or saline once NASH was established.

In both experimental models, treatment with hrAnxA1 improved parenchymal injury and lobular inflammation without interfering with the extension of steatosis. Furthermore, administration of hrAnxA1 significantly attenuated the hepatic expression of α1-procollagen and TGF-β1 and reduced collagen deposition, as evaluated by collagen Sirius Red staining. Flow cytometry and immunohistochemistry showed that hrAnxA1 did not affect the liver recruitment of macrophages, but strongly interfered with the formation of crown-like macrophage aggregates and reduced their capacity of producing pro-fibrogenic mediators like osteopontin (OPN) and galectin-3 (Gal-3). This effect was related to an interference with the acquisition of a specific macrophage phenotype characterized by the expression of the Triggering Receptor Expressed on Myeloid cells 2 (TREM-2), CD9 and CD206, previously associated with NASH evolution to cirrhosis.

Collectively, these results indicate that, beside ameliorating hepatic inflammation, AnxA1 is specifically effective in preventing NASH-associated fibrosis by interfering with macrophage pro-fibrogenic features. Such a novel function of AnxA1 gives the rationale for the development of AnxA1 analogs for the therapeutic control of NASH evolution.

Introduction

Nonalcoholic steatohepatitis (NASH) is now becoming one of the most common cause of end-stage liver disease in Western countries with a death rate ascribed to NASH-related cirrhosis accounting for 12–25% [1,2]. NASH is also an increasingly common cause of hepatocellular carcinoma (HCC) [3]. Besides hepatic injury, the presence of steatohepatitis also increases the prevalence of non-hepatic diseases such as type 2 diabetes mellitus, cardiovascular diseases, chronic kidney diseases and osteoporosis independently from the risk factors in common with metabolic syndrome [4]. In these settings, liver inflammation not only is the driving force for NASH evolution to cirrhosis, but also contributes to extrahepatic injury. Thus, targeting hepatic inflammation has become an important objective for the development of new treatments of NASH.

*These authors contributed equally to this work.
†These authors share the senior authorship.

Received: 30 November 2021
Revised: 07 April 2022
Accepted: 19 April 2022

Accepted Manuscript online: 19 April 2022
Version of Record published: 04 May 2022

Clinical Science (2022) **136** 643–656
https://doi.org/10.1042/CS20211122

Animal experiments and clinical trials have shown that interfering with pro-inflammatory cytokines/chemokines, leukocyte adhesion molecules or gut dysbiosis is effective in ameliorating lobular inflammation and NASH progression to fibrosis [5,6]. A different approach to control inflammation might rely on the use of physiological modulators that orchestrate the resolution of inflammatory processes and promote tissue healing [7]. Among these pro-resolving factors, Annexin A1 (AnxA1), also known as lipocortin-1, represents a possible candidate.

AnxA1 is a 37-kDa calcium–phospholipid-binding protein highly expressed in myeloid cells and regulated by glucocorticoids [8]. AnxA1 interaction with its receptor, formyl peptide receptor 2/lipoxin A4 receptor (FPR2/ALX), down-regulates the production of proinflammatory mediators, such as eicosanoids, nitric oxide and interleukin (IL)-6 (IL-6), reduces neutrophil migration to inflammatory sites, and promotes clearance of apoptotic granulocytes [8,9]. Furthermore, recent studies have shown that endogenous AnxA1 favors epithelial repair and muscle regeneration [9,10]. We have observed that AnxA1 is selectively up-regulated in macrophages from mouse and human NASH livers [11]. Moreover, in NASH patients hepatic AnxA1 transcripts show an inverse correlation with disease progression to fibrosis/cirrhosis [11]. Furthermore, AnxA1 deficiency enhances insulin resistance and metabolic impairment in mice receiving an obesogenic diet [12], while it worsens lobular inflammation and hepatic fibrosis in experimental NASH [11]. These latter effects associate with an enhanced macrophage recruitment as well as their pro-inflammatory M1 phenotype and activity [11]. Consistently, *in vitro* addition of recombinant AnxA1 to macrophages isolated from NASH livers reduces M1 polarization by stimulating the production of IL-10 [11]. In the same vein, AnxA1 supplementation improves insulin resistance and type 2 diabetes complications in mice fed a high-fat diet [12].

Based on these studies and the recent observations that AnxA1 and AnxA1 mimetic peptides are effective in improving inflammation in animal models of diabetic kidney damage and atherosclerosis [13,14], the present study investigated the possible application of AnxA1 in controlling steatohepatitis in mice with experimental NASH.

Materials and methods

Mice and experimental protocol

Wildtype C57BL/6 mice were housed in pathogen-free conditions and fed *ad libitum* with standard chow diet and water. Steatohepatitis was induced by feeding 8-week-old male mice with either a methionine–choline-deficient (MCD) diet for 2 or 8 weeks or with a high-fat/carbohydrate diet enriched with 1.25% cholesterol Western diet (WD) for 10–16 weeks (Laboratorio Dottori Piccioni, Gessate, Italy). Control animals received a diet supplemented by either choline/methionine or standard chow diet. Mice were treated for 5 days a week by daily intraperitoneal injection of human recombinant AnxA1 (hrAnxA1; 1 μg/daily in saline) according to a previously published protocol [14] that allowed effective pharmacokinetics and avoided production of neutralizing antibodies. Control animals received an injection of saline alone. At the end of the treatments, mice were anesthetized with sevoflurane, and after checking the anesthesia depth, the blood was collected by retro-orbital bleeding. Afterwards, the mice were killed by cervical dislocation. Animal experiments were performed at the animal facility of the Department of Health Sciences, University of East Piedmont (Novara, Italy) and complied with EU ethical guidelines for animal experimentation. The study protocols received ethical approval by the Italian Ministry of Health (authorization number 449/2019-PR) according to the European law requirements.

AnxA1 recombinant protein purification

cDNA of hrAnxA1 carrying a cleavable N-terminal poly-His tag was expressed in *Escherichia coli* and purified as previously reported [14]. The purity of recombinant AnxA1, was assessed by sodium dodecyl sulphate/polyacrylamide gel electrophoresis and matrix-assisted laser desorption/ionization dual time-of-flight mass spectrometry and was >95%.

Assessment of liver injury

Livers were rapidly removed, rinsed in ice-cold saline and cut in pieces. Aliquots were immediately frozen in liquid nitrogen and kept at −80°C until analysis. Two portions of the left lobe from each liver were fixed in 10% formalin for 24 h and embedded in paraffin. Plasma alanine aminotransferase (ALT) levels and liver triglycerides were determined by spectrometric kits supplied, respectively, by Gesan Production SRL (Campobello di Mazara, Italy) and Sigma Aldrich (Milano, Italy).

Histology and immunohistochemistry

Liver sections (4-μm-thick) were stained with Hematoxylin/Eosin using a Roche Ventana HE 600 automatic staining system (Roche Diagnostics International AG, Rotkreuz, Switzerland), while collagen deposition was detected

by Picro-Sirius Red staining. Sections were scored blindly for steatosis and lobular inflammation, as described [11]. The extension of Sirius Red was quantified by histo-morphometric analysis using the ImageJ software (https://imagej.nih.gov/ij/). To detect liver macrophages, tissue sections were stained in formalin-fixed sections using rabbit polyclonal antibodies against F4-80 and goat polyclonal antibodies against galectin-3 (Gal-3) provided by, respectively, Abcam (Cambridge, U.K.) and R&D Systems (Minneapolis, U.S.A.) in combination with a horseradish peroxidase polymer kit (Biocare Medical, Concord, CA, U.S.A.). Microphotographs were taken using a Nikon Eclips CI microscope fitted with 20 × 0.5 and 40 × 0.75 PlanFluor lens and a DSR12 camera (Nikon Europe BV, Amsterdam, Netherlands) through the NIS-Elements F4.60.00 acquisition software.

Flow cytometry analysis of liver leukocytes

Livers were digested by type IV collagenase (Worthington, U.S.A.), and intrahepatic leukocytes were isolated by multiple differential centrifugation steps according to [15]. The cell preparations were then subjected to red cell lysis by BD FACS™ Lysing Solution (BD Bioscience, San Jose, CA, U.S.A.) and stained using combinations of the following monoclonal antibodies: CD45 (Clone 30-F11, Cat. 12-0451-82), Ly6C (Clone HK1.4, Cat. 53-59-32-80), Ly6G (Clone Clone RB6-8C5, Cat. 47-5931-82,), MHCII (Clone M5/114.15.2, Cat. 56-5321-80), CD206 (Clone MR6F3, Cat. 25-2061-80), CD9 (MZ3FCRUO, Cat. 124815), C-type lectin-like receptor 2 (CLEC-2; 17D9/CLEC-2FCRUO, Cat. 146103), T-cell membrane protein 4 (TIM-4; RMT4-54FCRUO, Cat. 130019) eBioscience, (Thermo Fisher Scientific, Milano, Italy), CD11b (Clone M1/70, Cat. 101212), F4-80 (Clone BM8, Cat. 123113, Biolegend, San Diego, CA, U.S.A.), Triggering Receptor Expressed on Myeloid cells 2 (TREM-2; Clone 78.18, Cat. MA5-28223, Thermo Fisher Scientific, Milano, Italy). Sample analysis was performed using the Attune NxT flow cytometer (Thermo Fisher Scientific, Waltham, MA, U.S.A.) and data were elaborated with FlowJo™ Software (BD Biosciences, San Jose, CA, U.S.A.).

Metabolic assessment

After overnight fasting, mice received a single intraperitoneal injection of D-glucose (1.5 mg/g body weight in saline). Blood sampling was performed by tail vein incision with sterile needles and glycemia was measured by a glucometer (Menarini Diagnostics, Milan, Italy) before and after 10, 30, 60, 90 and 120 min of glucose administration.

mRNA extraction and real-time PCR

mRNA was extracted from snap-frozen liver fragments using the TRIzol™ Reagent (Thermo Fisher Scientific, Milano, Italy). cDNA was generated from 1 μg of mRNA using the High-Capacity cDNA Reverse Transcription Kit (Applied Biosystems Italia, Monza, Italy) in a Techne TC-312 thermocycler (TecneInc, Burlington NJ, U.S.A.). Real-time PCR was performed in a CFX96™ Real-time PCR System (Bio-Rad, Hercules, California, U.S.A.) using TaqMan Gene Expression Master Mix and TaqMan Gene Expression probes for mouse tumor necrosis factor-α (TNF-α; Mm99999068_m1), CCL2 (Mm00441242_m1), CD11b (Mm00434455_m1), CD163 (Mm00474091_m1), TREM-2 (Mm04209422_m1), MerTK (Mm00434920_m1), Gal-3 (Mm00802901_m1), osteopontin (OPN) (Mm01204014_m1), α1-procollagen (Mm00801666_g1), TGF-β1 (Mm00441724_m1) (Thermo Fisher Scientific, Milano, Italy) and β-actin (Cat. No. 4352663, Applied Biosystems Italia, Monza, Italy). All samples were run in duplicate and the relative gene expression, calculated as $2^{-\Delta C_t}$ over that of β-actin gene, was expressed as fold increase over the relative control samples.

Data analysis and statistical calculations

Statistical analyses were performed by SPSS statistical software (SPSS Inc. Chicago IL, U.S.A.) using one-way ANOVA test with Tukey's correction for multiple comparisons or Kruskal–Wallis test for non-parametric values. Significance was taken at the 5% level. Normality distribution was assessed by the Kolmogorov–Smirnov algorithm.

Results

The effects of hrAnxA1 on modifying the severity of NASH were preliminary evaluated in a set of experiments in which steatohepatitis was induced in C57BL/6 mice by feeding a methionine/choline deficient (MCD) diet. For these experiments, animals received the MCD diet for 4 weeks to allow the development of extensive steatohepatitis; then, they were injected with hrAnxA1 or saline for further 4 weeks, while maintaining the same diet. At the end of the treatment, liver histology and biochemical analysis showed that administration of hrAnxA1 significantly reduced the severity of liver injury (Figure 1A) as measured by ALT release (Figure 1B). No changes were evident in the scores for hepatic steatosis (2.2 ± 0.9 *vs.* 1.6 ± 0.6 arbitrary units; n=13; P=0.22) and in liver triglyceride content (Figure 1C). The same animals also showed a significant lowering in the histological scores for lobular inflammation (2.2 ±

Clinical Science (2022) **136** 643–656
https://doi.org/10.1042/CS20211122

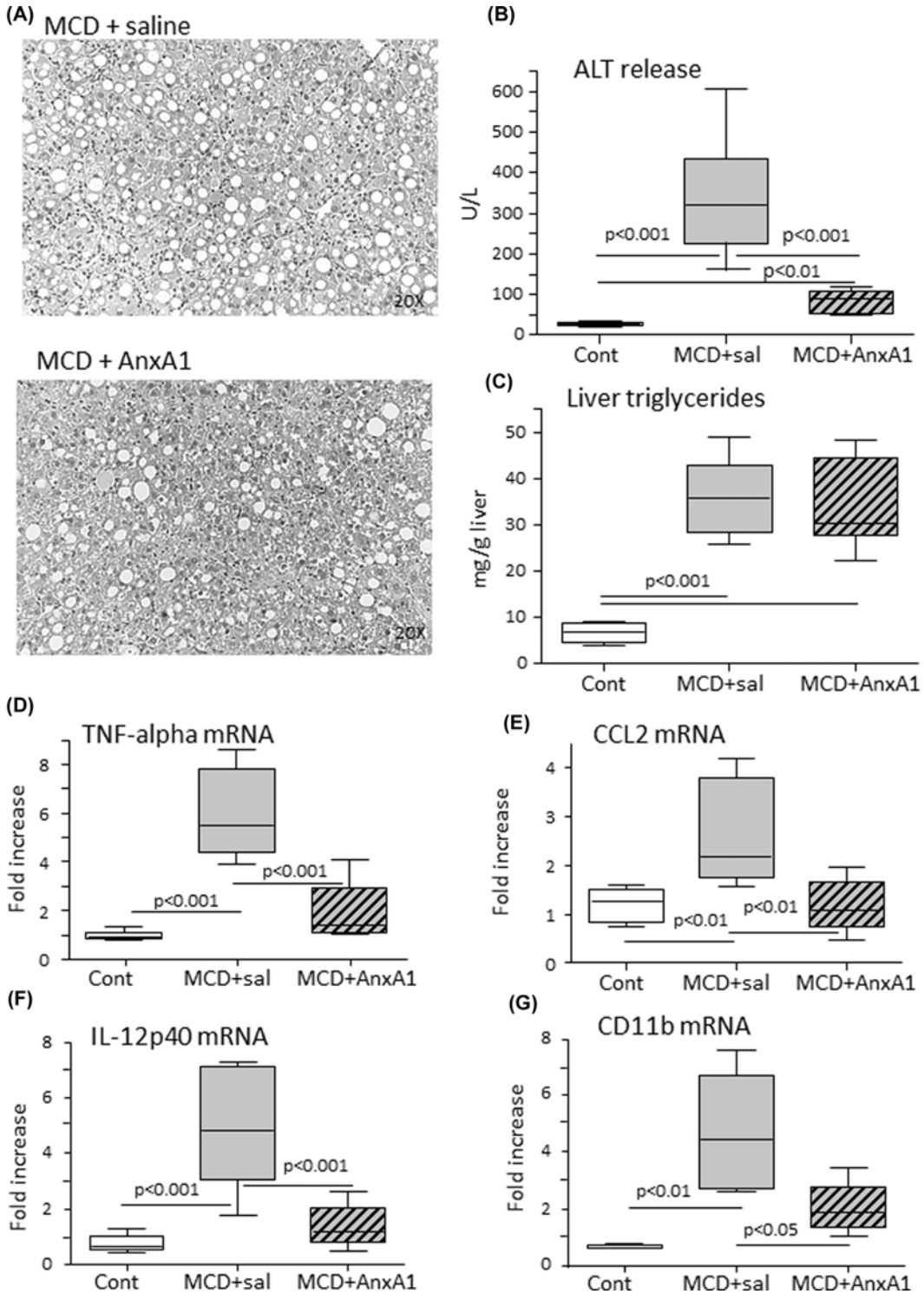

Figure 1. AnxA1 supplementation improves NASH-associated hepatic injury and inflammation in mice fed an MCD diet

NASH was induced in wildtype C57BL/6 mice by feeding MCD diet for 4 weeks. The animals were then randomly divided in two groups: one receiving AnxA1 (1 μg/daily in saline five times a week; MCD+AnxA1) and the other the same volume of saline (MCD+sal) and the administration of the MCD diet was continued for further 4 weeks. (**A**) Hematoxylin/Eosin staining of liver sections (magnification 20×). (**B**,**C**) ALT release and hepatic triglyceride content. (**D–G**) Hepatic transcripts of inflammatory markers TNF-α, CCL2, IL12p40 and CD11b as evaluated by RT-PCR. The values refer to six to eight animals per group and the boxes include the values within 25th and 75th percentile, while the horizontal bars represent the medians. The extremities of the vertical bars (10th–90th percentile) comprise 80% percent of the values.

0.8 *vs*. 0.8 ± 0.8 arbitrary units; n=13; P<0.05) as well as in the liver expression of pro-inflammatory markers like TNF-α, CCL2, IL-12p40 and the leukocyte marker integrin α M (ITGAM; CD11b) (Figure 1D–G). Steatohepatitis in mice receiving the MCD diet for 8 weeks increased liver transcripts for procollagen-1α and transforming growth factor 1β (TGF-1β) (Figure 2A–C) and the onset of liver fibrosis, as evidenced by intrahepatic collagen staining with Sirius Red (Figure 2D). Interestingly, mice treated with hrAnxA1 showed significant decrease in the transcripts for procollagen-1α and TGF-1β (Figure 2A–C), along with a lower Sirius Red staining, than those injected with saline alone (Figure 2D).

Although steatohepatitis induced by the MCD diet reproduces the inflammatory features of human NASH, this experimental model lacks metabolic derangements associated with obesity and insulin resistance that are common features of the human disease [16]. Furthermore, the development of fibrosis is usually modest in MCD-fed mice [16]. Thus, to better characterize the action of hrAnxA1 on the evolution from NASH to fibrosis, we switched to a nutritional model based on mice feeding with high-fat/carbohydrate diet enriched with 1.25% cholesterol known as Western diet (WD) [16].

To this aim, mice were fed with WD for 10 weeks to induce steatohepatitis before being randomized to receive hrAnxA1 supplementation. Preliminary experiments confirmed that 10 weeks feeding of mice with WD significantly increased body weight as compared with chow-fed controls and this was associated with an increase in liver weight due to intrahepatic fat accumulation (Supplementary Figure S1A). The presence of steatohepatitis was confirmed by histology (Supplementary Figure S1B) as well as by the elevation in the circulating levels of ALT (Supplementary Figure S1C) and in the liver transcripts for inflammatory markers (Supplementary Figure S1D,E). Although procollagen-1α mRNA was increased in the livers of WD-fed mice (Supplementary Figure S1F), histology did not detect changes in collagen deposition (Supplementary Figure S1G), suggesting that at this time point steatohepatitis has not led to marked fibrosis. Thus, 10-week WD-fed animals were a suitable experimental model to investigate whether treatment with hrANXA1 might interfere with NASH evolution to fibrosis.

Six weeks treatment with hrANXA1 (1 μg/g) of mice receiving WD did not appreciably modify body (33 ± 1.8 *vs*. 32.5 ± 2.6 g; n=12; P=0.7) and liver weights (2.3 ± 0.32 *vs*. 2.0 ± 0.32 g; n=12; P=0.12). As expected, 16-week WD feeding promoted the development of insulin resistance, as monitored through the glucose tolerance test (Supplementary Figure S2A). Nonetheless, the area under the curve (AUC) did not evidence an appreciable improvement of insulin response following administration of hrAnxA1 (Supplementary Figure S2B).

As observed in the animals receiving the MCD diet, hrANXA1 treatment of mice fed with WD improved liver histology (lobular inflammation score: 1.8 ± 0.4 *vs*. 0.8 ± 0.7 arbitrary units; n=12; P<0.05), transaminase release and expression of inflammatory markers (Figure 3), without affecting the extension of steatosis (2.0 ± 0.9 *vs*. 2.3 ± 0.8 arbitrary units; n=12; P=0.58). According to previous studies [16], WD administration led to diffuse hepatic fibrosis (Figure 2D–F).In these animals RT-PCR and Sirius Red collagen staining confirmed that hrANXA1 was effective in preventing the up-regulation in procollagen-1α and TGF-1β expression and almost abrogated intrahepatic collagen deposition (Figure 2D–F) as confirmed by morphometric evaluation of collagen Sirius Red staining areas (3.20 ± 0.93 *vs*. 0.35 ± 0.35%; n=23 fields; P<0.001).

Several reports have pointed on the capacity of ANXA1 to modulate macrophage functions by suppressing pro-inflammatory activities and stimulating pro-resolving functions [9,10]. In our hands, flow cytometry analysis of F4-80$^+$/CD11b$^+$ of hepatic macrophages showed that treatment with hrANXA1 did not interfere with their recruitment to the liver (Figure 4A). Similarly, the fraction of pro-inflammatory macrophages expressing the lymphocyte antigen 6 (Ly6C), also known as tissue plasminogen activator receptor [17], was not affected (Figure 4A). On the other hand, hrANXA1 reduced by ∼20% the prevalence of cell expressing the mannose-binding protein receptor (MRC1; CD206), a marker of reparative macrophages (Figure 4A).

Macrophages in human and rodent NASH livers are often characterized by the formation of aggregated containing enlarged cells with a foamy appearance due to the accumulation of cytoplasmic lipid droplets and cholesterol crystals reminiscent of crown-like structures detectable in the adipose tissue of obese subjects [18]. Immunohistochemistry for the macrophage marker F4-80 confirmed the presence of crown-like aggregates in the liver sections from mice fed WD for 16 weeks (Figure 5A). F4-80 immunostaining also showed that macrophages aggregates were greatly reduced by hrANXA1 treatment (Figure 5A).

In recent studies, single-cell RNA sequencing has revealed that macrophages expanding in either human or rodent NASH, have a specific phenotype, characterized by the expression of the TREM-2, CD63 and the glycoproteins CD9 and NMB (GPNMB). These cells, also called NASH-associated macrophages (NAMs), are the main components of crown-like macrophage aggregates [21] and their prevalence correlates with the severity of NASH [19], likely in relation to their capability of producing pro-fibrogenic mediators such as Osteopontin (OPN) and Galectin-3 (Gal-3) [19–22]. Since the worsening of NASH-associated fibrosis in AnxA1-deficient mice was characterized by an enhanced

Clinical Science (2022) **136** 643–656
https://doi.org/10.1042/CS20211122

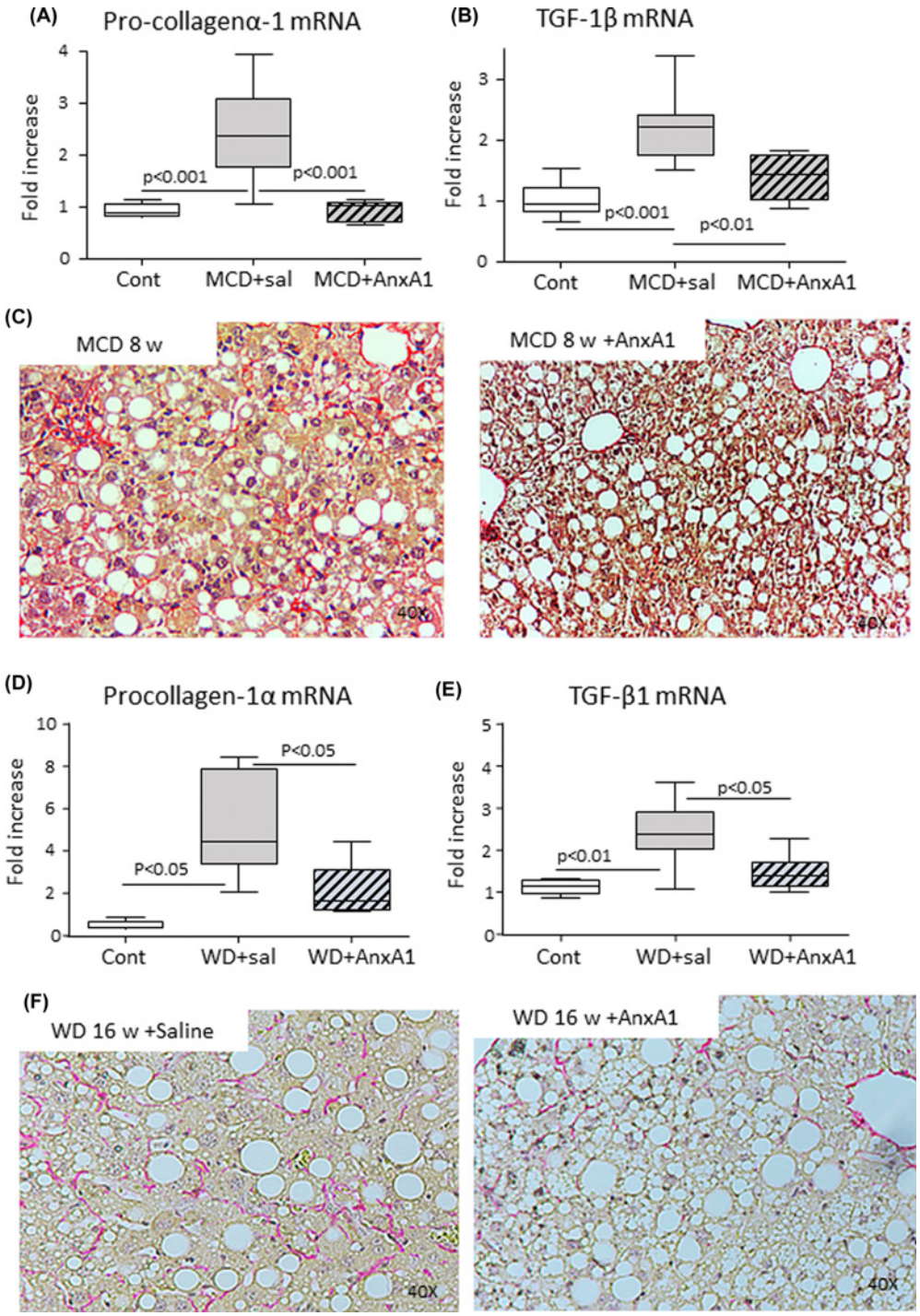

Figure 2. AnxA1 supplementation improves hepatic fibrosis in mice with NASH induced by feeding either an MCD diet or WD diet

NASH was induced in wildtype C57BL/6 mice by feeding MCD diet for 4 weeks or WD diet for 10 weeks. (**A–C**) The animals were randomly divided in two groups: one receiving AnxA1 (1 μg/daily in saline five times a week; MCD+AnxA1) and the other the same volume of saline (MCD+sal) and the administration of the MCD diet was continued for further 4 weeks. (**D–F**) The animals were divided to receive AnxA1 (1 μg/daily in saline five times a week; WD+AnxA1) or saline (WD+sal) and the administration of the WD diet was continued for further 6 weeks. The hepatic transcripts for procollagen-1α and TGF-β1 was evaluated by RT-PCR. Collagen deposition was evidenced by staining with Sirius Red (magnification 40×). The values refer to six to eight animals per group and the boxes include the values within 25th and 75th percentile, while the horizontal bars represent the medians. The extremities of the vertical bars (10th–90th percentile) comprise 80% percent of the values.

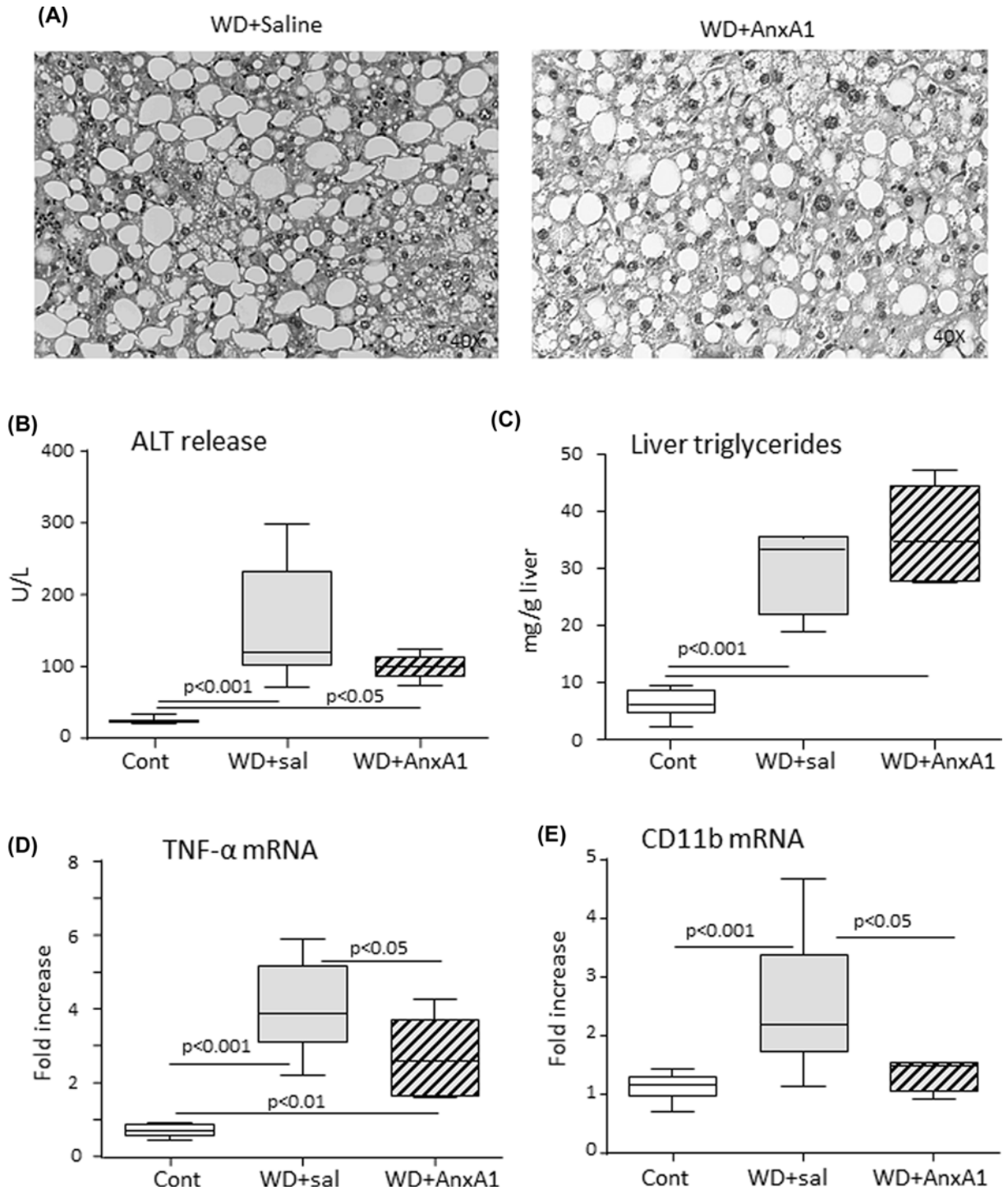

Figure 3. AnxA1 supplementation improves steatohepatitis in mice fed with WD

NASH was induced in wildtype C57BL/6 mice by feeding WD diet for 10 weeks. The animals were then randomly divided in two groups: one receiving AnxA1 (1 μg/daily in saline five times a week; WD+AnxA1) and the other the same volume of saline (WD+sal) and the administration of the diet was continued for further 6 weeks. (**A**) Hematoxylin/Eosin staining of liver sections (magnification 20×). (**B**,**C**) ALT release and hepatic triglyceride content. (**D**,**E**) The hepatic mRNA levels of inflammatory markers TNF-α and CD11b as evaluated by RT-PCR. The values refer to five to seven animals per group and the boxes include the values within 25th and 75th percentile, while the horizontal bars represent the medians. The extremities of the vertical bars (10th–90th percentile) comprise 80% percent of the values.

Clinical Science (2022) **136** 643–656
https://doi.org/10.1042/CS20211122

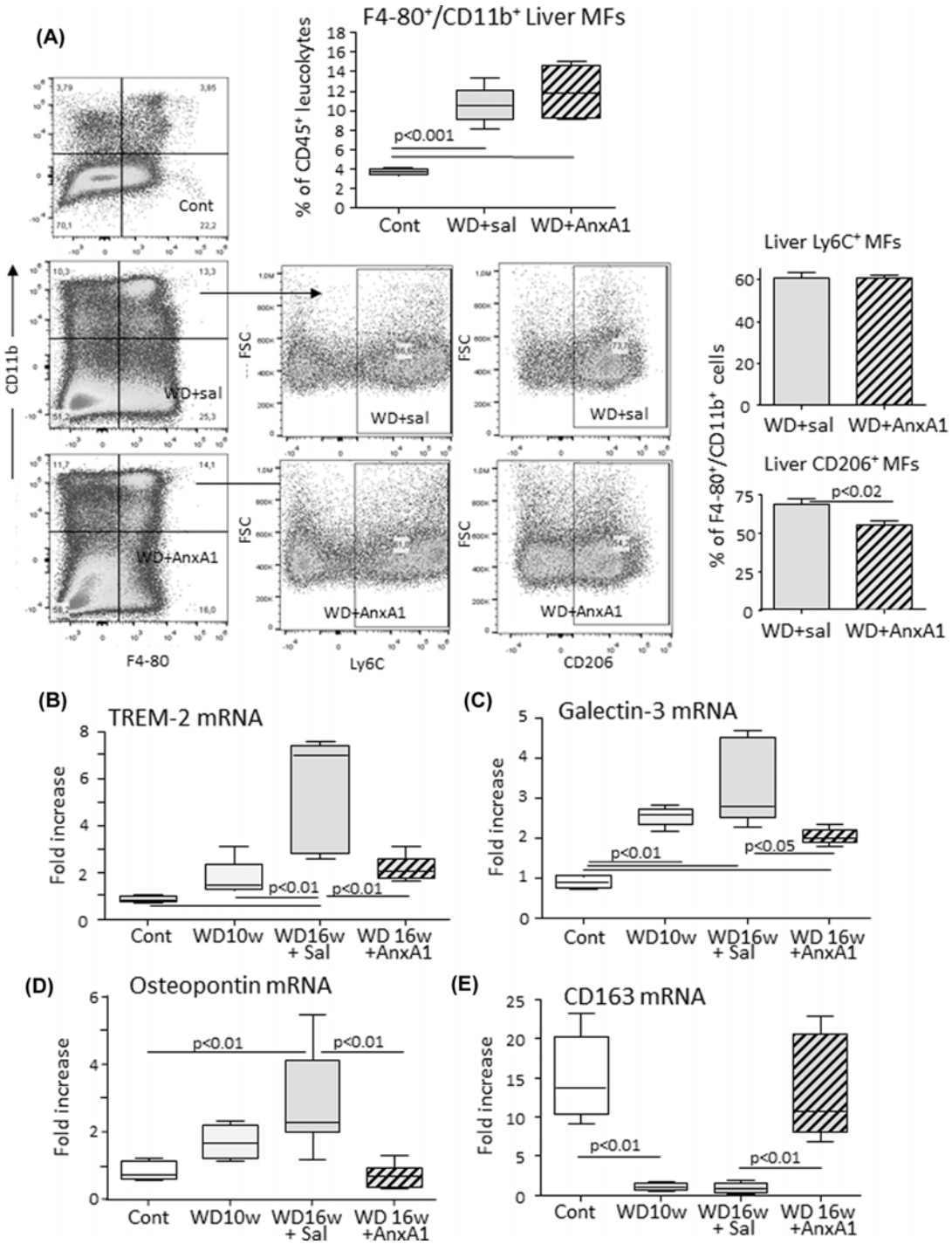

Figure 4. Effects of AnxA1 supplementation on the distribution and features of liver macrophages (MFs) infiltrating the liver of mice with WD-induced steatohepatitis

(**A**) The intrahepatic distribution of F4-80$^+$/CD11b$^+$ MFs and the relative prevalence of cells expressing Ly6C or CD206 was evaluated by flow cytometry in control mice (Cont) or mice receiving WD for 16 weeks in combination with either saline (WD-Sal) or AnxA1 treatment (WD+AnxA1). The values are means $\pm$ SD of three to four animals for each experimental group. (**B–E**) Changes in the hepatic transcripts of NASH-associated macrophage (NAM) markers TREM-2, Gal-3 and OPN along that of the Kupffer cell marker CD163 in mice receiving WD for 10 or 16 weeks in combination with either saline (WD-Sal) or AnxA1 treatment (WD+AnxA1). The liver mRNA levels were evaluated by RT-PCR in five to seven animals per group. The boxes include the values within 25th and 75th percentile, while the horizontal bars represent the medians. The extremities of the vertical bars (10th–90th percentile) comprise 80% percent of the values.

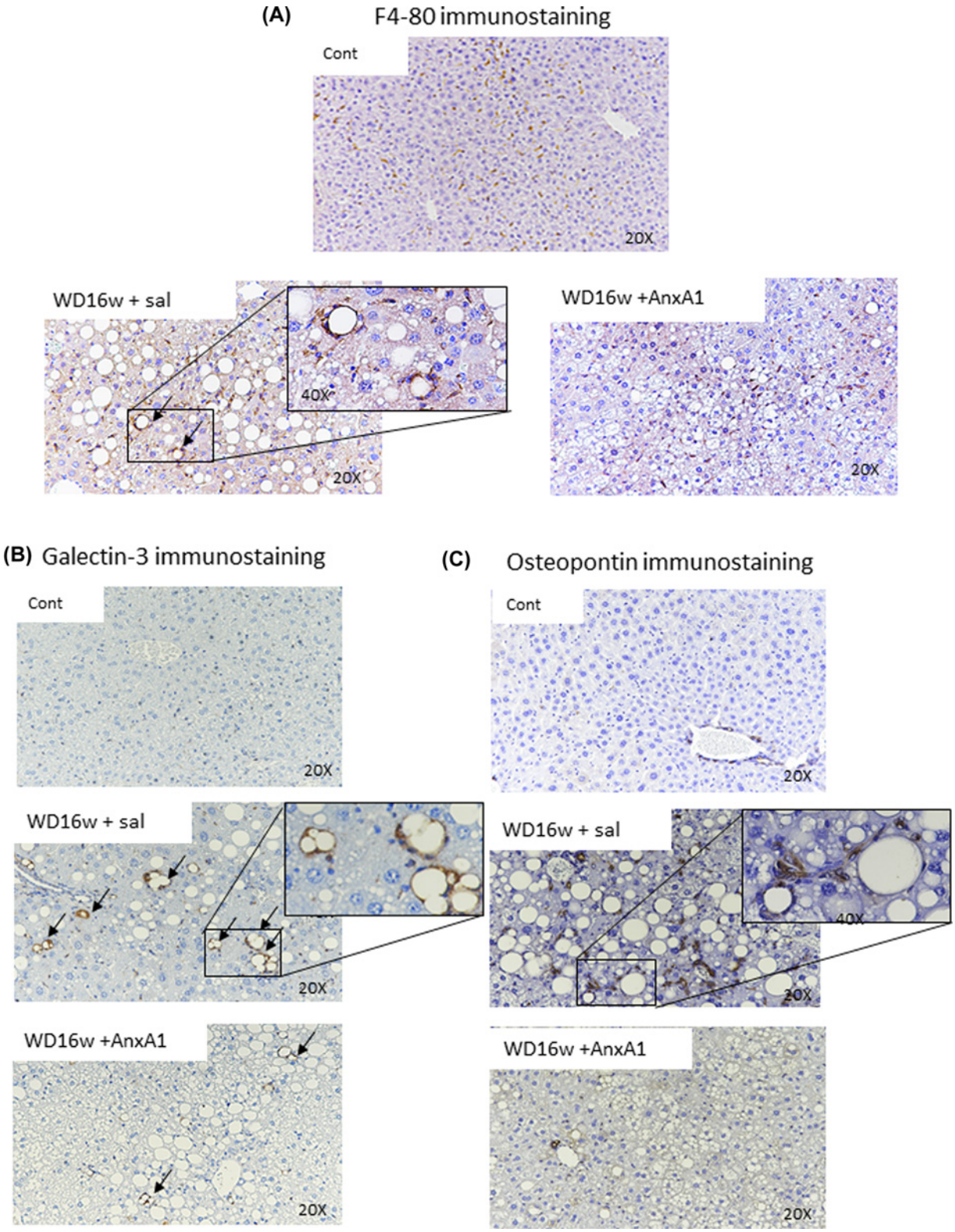

Figure 5. Effects of AnxA1 supplementation on the morphology of hepatic macrophages (MFs) and the production of Galectin-3 and Osteopontin

NASH was induced in wildtype C57BL/6 mice by feeding WD diet for 10 weeks. The animals were then randomly divided in two groups: one receiving AnxA1 (1 μg/daily in saline five times a week; WD+AnxA1) and the other the same volume of saline (WD+sal) and the diet was continued for further 6 weeks. (**A–C**) Liver macrophages immunostaining for, respectively, F4-80, Galectin-3 and Osteopontin (magnification 20×). The inserts show high magnification of the details of macrophages crown-like structures (arrows).

Clinical Science (2022) **136** 643–656
https://doi.org/10.1042/CS20211122

production of Gal-3 by macrophages in crown-like structures [11], in subsequent experiments we investigated the possibility that the protection against fibrosis observed in hrANXA1-treated mice might be related to an action on NAMs. Analysis of TREM-2, OPN and Gal-3 transcripts confirmed a strong up-regulation of these NAM markers in the livers of mice receiving WD that were effectively prevented by the administration of hrANXA1 (Figure 4B–D). Moreover, hrAnxA1 promoted the recovery in the expression of hemoglobin–haptoglobin scavenger receptor CD163 (Figure 4E), a marker of differentiated Kuppfer cells [20]. Immunohistochemistry for Gal-3 and OPN confirmed an increased staining for both mediators in NASH livers and showed that Gal-3 was selectively produced by macrophages within crown-like aggregates (Figure 5B), while OPN production was evident in both macrophages and ductular epithelial cells (Figure 5C). Again, the prevalence of both Gal-3 and OPN expressing cells was greatly reduced by the treatment with hrANXA1 (Figure 5B,C).

From these results, and previous observations showing that macrophages in crown-like aggregates in both rodent and human NASH produce AnxA1 [11,23], we postulated that AnxA1 might act in a paracrine manner in modulating the phenotype of hepatic macrophages. To verify such a possibility, we evaluated the effects of hrANXA1 on the differentiation of TREM-2^+/$CD9^+$ NAMs in mice receiving the MCD diet for 2 weeks. Preliminary experiments have shown that the early stages of steatohepatitis in these animals are accompanied by an expansion of F4-80^+/$CD11b^+$ macrophages which included ∼40% of cells that were $Ly6C^-$/TREM-2^+/$CD9^+$/$CD206^{high}$ (Supplementary Figure S3). In further experiments, during the second week on the MCD diet, mice were injected with hrANXA1 or saline for 5 days: herein, we observed that administration of hrANXA1 to mice did not affect the liver macrophages pool ($3.9 \pm 0.7 \times 10^5$ *vs*. $3.8 \pm 1.3 \times 10^5$ cells/g tissue; P=0.86), but significantly lowered the fraction of TREM-2^+/$CD206^+$ cells (Figure 6). This effect was accompanied by an increase in the prevalence of F4-80^+/$CD11b^+$ cells expressing the Kupffer cell markers CLEC-2 and the phosphatidylserine receptor TIM-4 ($0.45 \pm 0.05 \times 10^5$ *vs*. $0.55 \pm 0.06 \times 10^5$ cells/g tissue; P>0.05) and a parallel decrease in CLEC-2^-/TIM-4^- pool ($0.30 \pm 0.03 \times 10^5$ *vs*. $0.19 \pm 0.03 \times 10^5$ cells/g tissue; P>0.05) (Figure 6). No changes were instead observed in the fraction of CLEC-2^+/TIM-4^- ($1.3 \pm 0.4 \times 10^5$ *vs*. $2.7 \pm 1.1 \times 10^5$ cells/g tissue; P=0.42), supporting the possibility that hrANXA1 prevents NASH evolution to fibrosis by interfering with NAM phenotype in macrophages.

Discussion

As a result of the endemic presence of overweight and obesity in the Western world, nonalcoholic fatty liver disease (NAFLD) is becoming a leading cause of liver cirrhosis, with the prevalence of NAFLD-related end-stage liver diseases expected to further grow over the next decades [1]. On this latter respect, a prospective study in more than 400 patients, with biopsy-proven NAFLD with or without steatohepatitis, demonstrated that presence of NASH doubles the rate of disease progression to fibrosis [24]. Thus, targeting inflammation represents a key aspect for developing effective treatments for progressive NAFLD. In these settings, the interest for a possible therapeutic use of AnxA1 in NASH stems from the observation that the development of insulin resistance, lipid metabolism derangements, lobular inflammation and fibrosis are enhanced in AnxA1-deficient mice receiving either high-fat or MCD diets [11,12].

By using two different experimental models of NASH, we observed that treating mice with established steatohepatitis with hrAnxA1 not only attenuates liver damage and inflammation but also effectively prevents disease progression to fibrosis. The actions of AnxA1 appear unrelated to effects on metabolic control since, differently from what reported by Purvis and colleagues [12]; in our experimental settings, hrAnxA1 was ineffective in ameliorating liver steatosis and insulin resistance in mice receiving the WD. Such a discrepancy can be explained by the different experimental models. The high-fat diet used in Purvis' experiments causes a lower degree of hepatic inflammation than the cholesterol-enriched WD used in our work [15] and this might likely influence the severity of the derangements in lipid and glucose metabolism. Furthermore, the time frame between starting the diet and hrAnxA1 administration, was more than two-fold longer in our protocol, thus entailing the possibility of an at least partially effective recovery from liver fat accumulation.

The ability of AnxA1 to ameliorate NASH hepatic damage and inflammation is in-line with its recognized action in reducing granulocyte recruitment and macrophage M1 polarization [8,9,11]. Nonetheless, our results unveil that in NASH AnxA1 is also very effective in preventing disease progression to fibrosis. Such antifibrotic action is consistent with previous reports showing that AnxA1 or AnxA1 mimetic peptides improve lung fibrosis induced by bleomycin or silica particles [25,26]. In NASH livers, the antifibrotic function of hrAnxA1 does not involve changes in the number of hepatic macrophages but it rather associates with the modulation of their phenotype. Treatment with hrAnxA1, in fact, reduces the production of the profibrogenic mediator such Gal-3 and OPN that have been previously shown to contribute to liver fibrosis in NASH [27,28]. Moreover, hrAnxA1 affects macrophage capacity

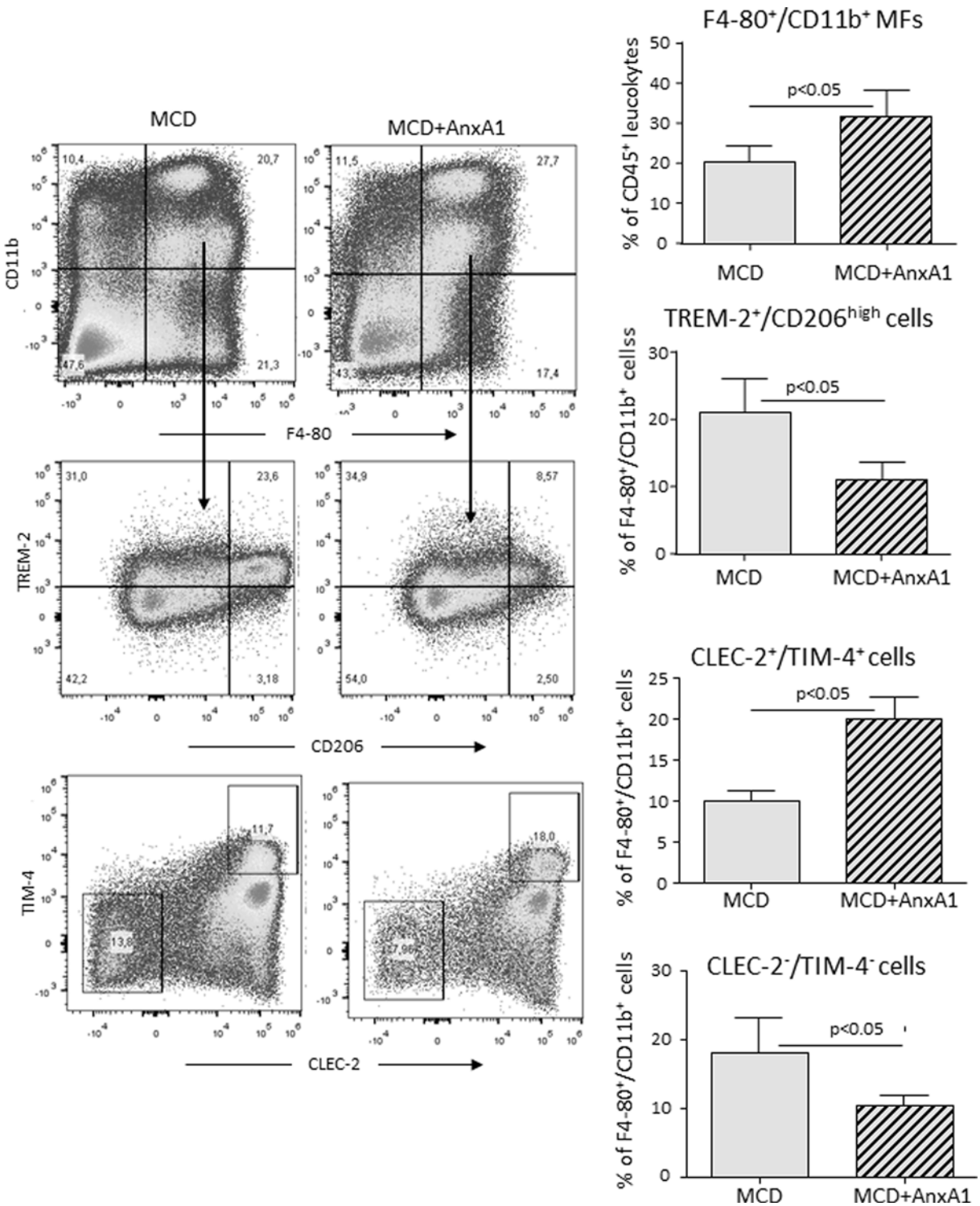

Figure 6. AnxA1 supplementation modulates the relative expression of NAM and Kupffer cell markers in liver macrophages (MFs) of mice with NASH

NASH was induced in wildtype C57BL/6 mice by feeding MCD diet for 2 weeks and during the second week the animals received AnxA1 for 5 days (1 μg/daily in saline; MCD+AnxA1) or the same volume of saline (MCD+sal). The intrahepatic distribution of F4-80⁺/CD11b⁺ MFs and the relative prevalence of cells expressing NAM markers TREM-2 and CD206 or Kupffer cell markers CLEC-2 and TIM-4 was evaluated by flow cytometry. The values are means ± SD of three to four animals for each experimental group.

Clinical Science (2022) **136** 643–656
https://doi.org/10.1042/CS20211122

of forming crown-like aggregates. The presence of clusters of enlarged and vacuolated macrophages, known as hepatic crown-like structures or lipogranulomas is a feature of both human and rodent NASH [29]. Previous studies have shown that these macrophages derive from liver-recruited monocytes and display pro-inflammatory activity [23,30,31]. In addition, these cells can sustain the fibrosis evolution of NASH in view of their colocalization with regions of stellate cell expansion [21,22]. So far, the mechanisms leading to the formation of crown-like structures in NASH have not been completely characterized. Studies by Ioannou and colleagues [32] have shown that macrophage phagocytosis of cholesterol crystals present in dying fat-laden hepatocytes promotes the formation of these crown-like structures. It is noteworthy that these macrophages are also the main producers of AnxA1 in both rodent and human NASH livers [11,23]. However, in NASH patients hepatic AnxA1 transcripts inversely correlate with the severity of fibrosis/cirrhosis [11], while activated hepatic stellate cells colocalize with Gal-3-positive crown-like structures in the livers of AnxA1-deficient mice with NASH [11]. This opens a strong possibility that endogenous AnxA1 might be involved in a juxtacrine/paracrine loop that regulates macrophage responses to stimuli, which promote crown-like aggregate formation and fibrogenic mediators' secretion.

Recent reports have outlined the heterogeneity of hepatic macrophages in NASH showing that during disease evolution, resident Kupffer cells are lost, and the liver is enriched by several subsets of monocyte-derived macrophages displaying different phenotypes [33]. In more detail, NASH in both rodents and humans is characterized by the abundance of $CD63^+/CD9^+/GPNMB^+/TREM\text{-}2^+$ NAMs [18–21], which have similarities with TREM-2/CD9-expressing lipid-associated macrophages (LAMs) detected in obese adipose tissue [34]. It is also noteworthy that NAMs contribute to the formation of crown-like aggregates [21]. The work by Ramachandran and colleagues [34] demonstrated that the TREM-2/CD9/OPN/Gal-3 signature also characterizes scar-associated macrophages identified in human fibrotic livers. Lineage tracking indicates that NAMs and scar-associated macrophages derive from liver infiltrating monocytes [21,35] and acquire their phenotype in response to specific signals in interstitial liver niche [19,36]. We have observed that beside interfering with OPN and Gal-3 gene expression, administration of AnxA1 affects the differentiation of $TREM\text{-}2^+/CD9^+$ macrophage while promoting the acquisition of Kupffer cell markers CLEC-2 and TIM-4. Indeed, the recent works have shown that during NASH progression liver infiltrating monocyte-derived macrophages can also acquire Kupffer cell-like features [21,37]. Although the role of these cells in NASH evolution are presently poorly characterized, our data suggest the possibility that AnxA1 can prevent the development of fibrosis in NASH by skewing liver macrophage differentiation from pro-fibrogenic NAMs to a phenotype reminiscent that of monocyte-derived Kupffer cells.

Conclusions

These results unveil a novel functional role for AnxA1 in NASH progression by demonstrating its property of interfering with the development of a specific macrophage phenotype associated with the progression of steatohepatitis to fibrosis. Such a novel function of AnxA1 provides a strong rationale for the application of AnxA1, or AnxA1 analogs, to achieve therapeutic control of NASH evolution.

Clinical perspectives

- AnxA1 is a protein mediator involved in the resolution of inflammation that has been implicated in modulating hepatic inflammation in NASH.
- We show here that the treatment with hrAnxA1 not only improves parenchymal injury and lobular inflammation in two mice experimental models of NASH but is very effective in preventing the development of liver fibrosis. This effect appears related to AnxA1 capacity of interfering with the development of a specific macrophage phenotype associated with the progression of steatohepatitis to fibrosis.
- Such a novel function of AnxA1 gives the rational for the development of AnxA1 analogues for the therapeutic control of NASH evolution.

Data Availability

The raw data supporting the conclusions of this article will be made available by the authors, without undue reservation.

PORTLAND PRESS

Competing Interests

Mauro Perretti is on the Scientific Advisory Board of ResoTher Pharma AS, which is developing AnxA1-derived peptides for cardiovascular settings. He also consults for Bristol Myers Squibb, SynAct Pharma and TXP Pharma.
The authors declare that there are no competing interests associated with the manuscript.

Funding

This work was supported by the unrestricted grant from the ResoTher Pharma ApS (Holte, Denmark); the University of East Piedmont (FAR Grants 2017 and Project of Excellence FOHN); the William Harvey Research Foundation (London, United Kingdom).

CRediT Author Contribution

Laila Lavanya Gadipudi: Formal analysis, Investigation, Methodology. **Naresh Naik Ramavath:** Formal analysis, Investigation, Methodology. **Alessia Provera:** Formal analysis, Investigation, Methodology. **Chris Reutelingsperger:** Resources, Writing—review & editing. **Emanuele Albano:** Conceptualization, Funding acquisition, Writing—original draft, Writing—review & editing. **Mauro Perretti:** Conceptualization, Supervision, Writing—review & editing. **Salvatore Sutti:** Conceptualization, Supervision, Methodology, Writing—review & editing.

Abbreviations

ALT, alanine aminotransferase; AnxA1, Annexin A1; CLEC-2, C-type lectin-like receptor 2; Gal-3, galectin-3; hr, human recombinant; IL, interleukin; IP, intraperitoneal; Ly6C, lymphocyte antigen 6; MCD, methionine–choline deficient; NAFLD, nonalcoholic fatty liver disease; NAM, NASH-associated macrophage; NASH, nonalcoholic steatohepatitis; OPN, osteopontin; TGF-1β, transforming growth factor 1β; TIM-4, T-cell membrane protein 4; TNF-α, tumor necrosis factor-α; TREM-2, triggering receptor expressed on myeloid cells 2; WD, Western diet.

References

1 Younossi, Z., Anstee, Q.M., Marietti, M., Hardy, T., Henry, L., Eslam, M. et al. (2018) Global burden of NAFLD and NASH: trends, predictions, risk factors and prevention. *Nat. Rev. Gastroenterol. Hepatol.* **15**, 11–20, https://doi.org/10.1038/nrgastro.2017.109
2 Lindenmeyer, C.C. and McCullough, A.J. (2018) The natural history of nonalcoholic fatty liver disease -an evolving view. *Clin. Liver Dis.* **22**, 11–21, https://doi.org/10.1016/j.cld.2017.08.003
3 Younes, R. and Bugianesi, E. (2018) Should we undertake surveillance for HCC in patients with NAFLD? *J. Hepatol.* **68**, 326–334, https://doi.org/10.1016/j.jhep.2017.10.006
4 Amstrong, M.J., Adams, L.A., Canbay, A. and Syn, W.K. (2014) Extrahepatic complications of nonalcoholic fatty liver disease. *Hepatology* **59**, 1174–1197, https://doi.org/10.1002/hep.26717
5 Rotman, Y. and Sanyal, A.J. (2017) Current and upcoming pharmacotherapy for non-alcoholic fatty liver disease. *Gut* **66**, 180–190, https://doi.org/10.1136/gutjnl-2016-312431
6 Reimer, K.C., Wree, A., Roderburg, C. and Tacke, F. (2020) New drugs for NAFLD: lessons from basic models to the clinic. *Hepatol Int.* **14**, 8–23, https://doi.org/10.1007/s12072-019-10001-4
7 Serhan, C.N. (2017) Treating inflammation and infection in the 21st century: new hints from decoding resolution mediators and mechanisms. *FASEB J.* **31**, 1273–1288, https://doi.org/10.1096/fj.201601222R
8 Sugimoto, M.A., Vago, J.P., Teixeira, M.M. and Sousa, L.P. (2016) Annexin A1 and the resolution of inflammation: modulation of neutrophil recruitment, apoptosis, and clearance. *J. Immunol. Res.* **2016**, 8239258, https://doi.org/10.1155/2016/8239258
9 Sheikh, M.H. and Solito, E. (2018) Annexin A1: uncovering the many talents of an old protein. *Int. J. Mol. Sci.* **19**, 1045, https://doi.org/10.3390/ijms19041045
10 McArthur, S., Juban, G., Gobbetti, T., Desgeorges, T., Theret, M., Gondin, J. et al. (2020) Annexin A1 drives macrophage skewing to accelerate muscle regeneration through AMPK activation. *J. Clin. Invest.* **130**, 1156–1167, https://doi.org/10.1172/JCI124635
11 Locatelli, I., Sutti, S., Jindal, A., Vacchiano, M., Bozzola, C., Reutelingsperger, C. et al. (2014) Endogenous annexin A1 is a novel protective determinant in nonalcoholic steatohepatitis in mice. *Hepatology* **60**, 531–544, https://doi.org/10.1002/hep.27141
12 Purvis, G.S.D., Collino, M., Loiola, R.A., Baragetti, A., Chiazza, F., Brovelli, M. et al. (2019) Identification of AnnexinA1 as an endogenous regulator of RhoA, and its role in the pathophysiology and experimental therapy of type-2 diabetes. *Front. Immunol.* **27**, 571, https://doi.org/10.3389/fimmu.2019.00571
13 Wu, L., Liu, C., Chang, D.Y., Zhan, R., Sun, J., Cui, S.H. et al. (2021) Annexin A1 alleviates kidney injury by promoting the resolution of inflammation in diabetic nephropathy. *Kidney Int.* **100**, 107–121, https://doi.org/10.1016/j.kint.2021.02.025
14 Kusters, D.H.M., Chatrou, M.L., Willems, B.A.G., De Saint-Hubert, M., Bauwens, M., van der Vorst, E. et al. (2015) Pharmacological treatment with annexin A1 reduces atherosclerotic plaque burden in LDLR-/- mice on Western type diet. *PLoS ONE* **10**, e0130484, https://doi.org/10.1371/journal.pone.0130484
15 Wiede, F. and Tiganis, T. (2018) Isolation and characterization of mouse intrahepatic lymphocytes by flow cytometry. *Methods Mol. Biol.* **1725**, 301–311, https://doi.org/10.1007/978-1-4939-7568-6˙23
16 Santhekadur, P.K., Kumar, D.P. and Sanyal, A.J. (2018) Preclinical models of non-alcoholic fatty liver disease. *J. Hepatol.* **68**, 230–237, https://doi.org/10.1016/j.jhep.2017.10.031

Clinical Science (2022) **136** 643–656
https://doi.org/10.1042/CS20211122

17 Wen, Y., Lambrecht, J., Ju, C. and Tacke, F. (2021) Hepatic macrophages in liver homeostasis and diseases-diversity, plasticity and therapeutic opportunities. *Cell Mol. Immunol.* **18**, 45–56, https://doi.org/10.1038/s41423-020-00558-8
18 Itoh, M., Kato, H., Suganami, T., Konuma, K., Marumoto, Y., Terai, S. et al. (2013) Hepatic crown-like structure: a unique histological feature in non-alcoholic steatohepatitis in mice and humans. *PLoS ONE* **8**, e82163, https://doi.org/10.1371/journal.pone.0082163
19 Xiong, X., Kuang, H., Ansari, S., Liu, T., Gong, J., Wang, S. et al. (2019) Landscape of intercellular crosstalk in healthy and NASH liver revealed by single-cell secretome gene analysis. *Mol. Cell* **75**, 644.e5–660.e5, https://doi.org/10.1016/j.molcel.2019.07.028
20 Seidman, J.S., Troutman, T.D., Sakai, M., Gola, A., Spann, N.J., Bennett, H. et al. (2020) Niche-specific reprogramming of epigenetic landscapes drives myeloid cell diversity in nonalcoholic steatohepatitis. *Immunity* **52**, 1057.e7–1074.e7, https://doi.org/10.1016/j.immuni.2020.04.001
21 Remmerie, A., Thoné, T., Castoldi, A., Seurinck, R., Pavie, B., Roels, J. et al. (2020) Osteopontin expression identifies a subset of recruited macrophages distinct from kupffer cells in the fatty liver. *Immunity* **53**, 641–657, https://doi.org/10.1016/j.immuni.2020.08.004
22 Daemen, S., Gainullina, A., Kalugotla, G., He, L., Chan, M.M., Beals, J.W. et al. (2021) Dynamic shifts in the composition of resident and recruited macrophages influence tissue remodeling in NASH. *Cell Rep.* **34**, 108626, https://doi.org/10.1016/j.celrep.2020.108626
23 Jindal, A., Bruzzì, S., Sutti, S., Locatelli, I., Bozzola, C., Paternostro, C. et al. (2015) Fat-laden macrophages modulate lobular inflammation in nonalcoholic steatohepatitis (NASH). *Exp. Mol. Pathol.* **99**, 155–162, https://doi.org/10.1016/j.yexmp.2015.06.015
24 Singh, S., Allen, A.M., Wang, Z., Prokop, L.J., Murad, M.H. and Loomba, R. (2015) Fibrosis progression in nonalcoholic fatty liver vs nonalcoholic steatohepatitis: a systematic review and meta-analysis of paired-biopsy studies. *Clin. Gastroenterol. Hepatol.* **13**, 643–654, https://doi.org/10.1016/j.cgh.2014.04.014
25 Trentin, P.G., Ferreira, T.P., Arantes, A.C., Ciambarella, B.T., Cordeiro, R.S., Flower, R.J. et al. (2015) Annexin A1 mimetic peptide controls the inflammatory and fibrotic effects of silica particles in mice. *Br. J. Pharmacol.* **172**, 3058–3071, https://doi.org/10.1111/bph.13109
26 Damazo, A.S., Sampaio, A.L., Nakata, C.M., Flower, R.J., Perretti, M. and Oliani, S.M. (2011) Endogenous annexin A1 counter-regulates bleomycin-induced lung fibrosis. *BMC Immunol.* **12**, 59, https://doi.org/10.1186/1471-2172-12-59
27 Henderson, N.C., Mackinnon, A.C., Farnworth, S.L., Poirier, F., Russo, F.P., Iredale, J.P. et al. (2006) Galectin-3 regulates myofibroblast activation and hepatic fibrosis. *Proc. Natl. Acad. Sci. U.S.A.* **103**, 5060–5065, https://doi.org/10.1073/pnas.0511167103
28 Syn, W.K., Choi, S.S., Liaskou, E., Karaca, G.F., Agboola, K.M., Oo, Y.H. et al. (2011) Osteopontin is induced by hedgehog pathway activation and promotes fibrosis progression in nonalcoholic steatohepatitis. *Hepatology* **53**, 106–115, https://doi.org/10.1002/hep.23998
29 Itoh, M., Kato, H., Suganami, T., Konuma, K., Marumoto, Y., Terai, S. et al. (2013) Hepatic crown-like structure: a unique histological feature in non-alcoholic steatohepatitis in mice and humans. *PLoS ONE* **8**, e82163, https://doi.org/10.1371/journal.pone.0082163
30 Leroux, A., Ferrere, G., Godie, V., Cailleux, F., Renoud, M.L., Gaudin, F. et al. (2012) Toxic lipids stored by Kupffer cells correlates with their pro-inflammatory phenotype at an early stage of steatohepatitis. *J. Hepatol.* **57**, 141–149, https://doi.org/10.1016/j.jhep.2012.02.028
31 Ioannou, G.N., Haigh, W.G., Thorning, D. and Savard, Ch. (2013) Hepatic cholesterol crystals and crown-like structures distinguish NASH from simple steatosis. *J. Lipid Res.* **54**, 1326–1334, https://doi.org/10.1194/jlr.M034876
32 Horn, C.L., Morales, A.L., Savard, C., Farrell, G.C. and Ioannou, G.N. (2022) Role of cholesterol-associated steatohepatitis in the development of NASH. *Hepatol. Commun.* **6**, 12–35, https://doi.org/10.1002/hep4.1801
33 Wen, Y., Lambrecht, J., Ju, C. and Tacke, F. (2021) Hepatic macrophages in liver homeostasis and diseases-diversity, plasticity and therapeutic opportunities. *Cell Mol. Immunol.* **18**, 45–56, https://doi.org/10.1038/s41423-020-00558-8
34 Jaitin, D.A., Adlung, L., Thaiss, C.A., Weiner, A., Li, B., Descamps, H. et al. (2019) Lipid-associated macrophages control metabolic homeostasis in a Trem2-dependent manner. *Cell* **178**, 686–698, https://doi.org/10.1016/j.cell.2019.05.054
35 Ramachandran, P., Dobie, R., Wilson-Kanamori, J.R., Dora, E.F., Henderson, B.E.P., Luu, N.T. et al. (2019) Resolving the fibrotic niche of human liver cirrhosis at single cell level. *Nature* **575**, 512–518, https://doi.org/10.1038/s41586-019-1631-3
36 Sakai, M., Troutman, T.D., Seidman, J.S., Ouyang, Z., Spann, N.J., Abe, Y. et al. (2019) Liver-derived signals sequentially reprogram myeloid enhancers to initiate and maintain Kupffer cell identity. *J. Immunity* **51**, 655–670, https://doi.org/10.1016/j.immuni.2019.09.002
37 Tran, S., Baba, I., Poupel, L., Dussaud, S., Moreau, M., Gélineau, A. et al. (2020) Impaired Kupffer cell self-renewal alters the liver response to lipid overload during non-alcoholic steatohepatitis. *Immunity* **53**, 627.e5–640.e5, https://doi.org/10.1016/j.immuni.2020.06.003